ISSN 2618-1584 Vol. 7, Issue 5: 29-42, DOI: 10.25236/FMSR.2025.070505

Construction and Validation of a Necroptosis-Related Gene Signature Associated with the Tumor Microenvironment in Melanoma

Yanqing Wang[1,a], Xianghui Meng[2,b], Ke Yang[3,c], Juhua Zhao[1,d,*]

[1]*Department of Dermatology, Beijing Anzhen Nanchong Hospital of Capital Medical University & Nanchong Central Hospital, Nanchong, China*
[2]*Department of Dermatology, Hongqi Hospital Affiliated to Mudanjiang Medical College, Mudanjiang, China*
[3]*Department of Plastic & Cosmetic Surgery, Guangxi Medical University, Nanning, China*
[a]*yanqing99992025@163.com,* [b]*xianghui777@126.com,* [c]*1015695862@qq.com,*
[d]*zhao08272024@163.com*
[*]*Corresponding author*

Abstract: *This study aimed to explore the prognostic value of necroptosis-related genes (NPRGs) in melanoma. A prognostic signature based on six NPRGs was constructed using the least absolute shrinkage and selection operator (LASSO) regression in the training cohort from The Cancer Genome Atlas (TCGA), with validation using the Gene Expression Omnibus (GEO) database (GSE65904). Patients were divided into high-risk and low-risk groups, and overall survival (OS) was compared using the Kaplan-Meier method. Cox regression analysis assessed the impact of clinicopathological features and risk scores on survival outcomes. The immune microenvironment was evaluated using the CIBERSORT method, and the relationship between clinical features, checkpoint gene expression, and risk scores was examined by correlation analysis. Gene expression of the six NPRGs was validated using the GEPIA2 database and immunohistochemistry (IHC). The prognostic signature predicted worse OS in the high-risk group, and this was confirmed in the validation cohort. Risk scores were found to independently predict survival in melanoma patients. Significant differences in the immune microenvironment and checkpoint gene expression were observed between risk groups. The necroptosis score showed a positive correlation with natural killer cells and M2 macrophages, and a negative correlation with T-cell and B-cell infiltration. Lower levels of immune checkpoint gene expression were observed in the high-risk group. IHC results confirmed the gene expression trends of NPRGs from the GEPIA2 database. In conclusion, the prognostic signature based on NPRGs can serve as a novel prognostic predictor in melanoma patients and reflect the immune microenvironment.*

Keywords: *Melanoma; Prognosis Signature; Tumor Immune Microenvironment; Necroptosis*

1. Introduction

Melanoma is a malignant tumor that originates from melanocytes. Of all malignant tumors, malignant melanoma accounts for about 5% of cases[1]. Since melanoma is one of the most malignant cancers known to humans, its incidence has risen globally for the past 50 years[2]. Therefore, early detection and treatment are crucial to enhance the prognosis of patients.

Necroptosis is a form of programmed inflammatory cell death mediated by RIP1, RIP3, and MLKL[3]. An oligomeric complex comprising FADD, caspase-8, and caspase-10 recruits active RIPK1. The RIP Potosome is created by RIPK1 phosphorylating RIPK3 without caspase-8. MLKL is then phosphorylated to create the necrosome. The MLKL oligomer translocates to PIP-rich patches in the plasma membrane. It makes macropores that allow ion inward flow, cell enlargement, and membrane lysis, followed by the uncontrolled release of intracellular substances, resulting in necrotic cell death[4]. According to reports, necroptosis typically has tumor-suppressive effects[5, 6]. Some necroptosis cells, however, were unable to fully account for the anticancer effects of necrosis-inducing substances, indicating a possible connection between necroptosis and antitumor immunity[7]. Understanding if necroptosis has a tissue-specific function in carcinogenesis and whether it has pro- or antitumor effects in various cancer types could open up new avenues for cancer therapy.

ISSN 2618-1584 Vol. 7, Issue 5: 29-42, DOI: 10.25236/FMSR.2025.070505

The precise part necroptosis plays in melanoma growth is still up for debate. This research set out to identify a predictive profile for necroptosis-related genes (NPRGs), evaluate the relationship between necroptosis and the tumor immunological microenvironment (TME), and examine the therapeutic benefits of immunotherapy and targeted therapy.

2. Materials and methods

2.1 Raw data acquisition and processing

389 human melanoma samples' transcriptome RNA sequences (FPKM value) and the corresponding clinical information were obtained from The Cancer Genome Atlas (TCGA; https://tcga-data.nci.nih.gov/tcga/) platform. The Gene Expression Omnibus (GEO) platform provided the melanoma samples for the GEO cohort (GSE65904) (n = 214). The 67 original NPRGs used in this study were compiled from published studies, and the specific list can be found in the relevant literature.The FPKM values in the TCGA melanoma were transformed to Transcripts Per Kilobase Million (TPM) values, and samples with inadequate clinical data (age, gender, stage, overall survival [OS] time, etc.) were removed[8]. The Masked Somatic Mutation data (Varscan. Somatic. Maf) from the TCGA database was used to compute mutation frequency.

2.2 Construction of the NPRGs prognostic signature

To find suitable modeling genes from NPRGs, the "glmnet" package in R used LASSO regression. Based on the optimal value of the penalty parameter (λ), relevant modeling genes and their coefficients were kept. The sum of the coefficient values was then multiplied by the expression of the genes to create an NPRGs prognostic signature.

2.3 Validation of the NPRGs prognostic signature

Each melanoma patient in the TCGA and GEO groups was assigned a risk score based on the prognostic signature and divided into high- or low-risk groups using the median value. Kaplan-Meier survival curves and a log-rank test assessed survival differences. The "pheatmap" package in R generated a heat map to show NPRG expression levels in the two groups. ROC curve analysis with the "survival," "survminer," and "timeROC" packages evaluated the signature's specificity, sensitivity, and predictive accuracy (AUC). Scatter plots and risk score distributions were used to illustrate the relationships between death states and risk scores.

2.4 NPRGs prognostic signature and other clinical features correlations

From the TCGA platform, we retrieved the mutation data related to melanoma cases. The mutations between high-risk and low-risk groups were analyzed using the "maftool" package in R[9]. The OS between patients with high and low tumor mutation burden (TMB) and TMB combined with necroptosis scores were then evaluated. Also examined was the relationship between necroptosis scores and other clinical traits (age, stage, and gender).

2.5 Independent prognostic analysis of the necroptosis scores

To further explore the relationships between the necroptosis scores and clinicopathological features, we integrated the clinicopathological data with the necroptosis scores of the patients. The "survival" package in R was used to perform univariate and multivariate Cox proportional hazards regression analysis to test if the prognostic signature's predictive power was independent of clinicopathological traits. The results of the univariate and multivariate Cox analyses were visualized using the "forestplot" package in R.

2.6 Nomogram Model Establishment

A nomogram was constructed by combining the necroptosis scores with other clinical features. The sum of each patient's points was determined based on the nomogram. The calibration curves were used to contrast the anticipated probability of a 1-, 3-, and 5-year survival time by the nomogram with the actual survival time.

ISSN 2618-1584 Vol. 7, Issue 5: 29-42, DOI: 10.25236/FMSR.2025.070505

2.7 Profile of tumor-infiltrating immune cells (TICs) in melanoma patients

The relative proportion of 22 immune cells was assessed using the CIBERSORT (https://cibersort.stanford.edu) algorithm in melanoma patients. The simulation calculation was 1000 times run based on the gene expression profile of 22 immune cell subtypes. Finally, it was possible to determine the relative composition ratio of the 22 immune cells in each sample.

2.8 Exploration of the associations of the risk score with targets of targeted therapy and immunotherapy

The relationships between the necroptosis scores and therapy-related targets were assessed using Pearson's correlation analysis. The "ggpubr" package in R was used to draw those relationships, and the Wilcoxon rank-sum test was used to see whether there was a difference.

2.9 Validation of the expression levels of six NPRGs

The mRNA expression levels of NPRGs were analyzed using the GEPIA2 database (http://gepia2.cancer-pku.cn/). Immunohistochemical assays validated the protein expression levels of NPRGs. Melanoma and adjacent tissues for immunohistochemistry were provided by The First Affiliated Hospital of Guangxi Medical University, with melanoma confirmed by pathology. Clinicopathological data, including age and sex, were collected.

Tissue sections were submerged in xylene for 20 minutes, followed by a fresh xylene treatment. The dewaxed sections were immersed in distilled water for 5 minutes, then in 95%, 80%, and 100% ethanol for 5 minutes each. Antigen retrieval was performed using alkaline Tri-EDTA solution (pH 9) heated in a pressure cooker for 2 minutes, followed by cooling to room temperature. Sections were then exposed to 3% H2O2 in the dark for 10 minutes, blocked with sheep serum for 30 minutes, and incubated overnight with primary antibody RP215 at 4°C. Afterward, secondary antibody with HRP was applied at room temperature for 30 minutes. Color development was done using diaminobenzidine (DAB), followed by hematoxylin counterstaining.

Ten high-power (400x) fields were randomly selected, and images were reviewed independently by two researchers. The cell nuclei stained blue with hematoxylin, while positive DAB staining appeared brownish-yellow.

2.10 Statistical analysis

The Wilcoxon rank-sum test was used to compare the two groups in question. The Kruskal-Wallis test was used for comparisons involving three or more groups. Survival analyses, including necroptosis scores, were carried out using the Kaplan-Meier method. Using the log-rank test, the difference in the survival statistic was examined. $P < 0.05$ was considered statistically significant for all data analyses, which were carried out using R software version 4.0.2.

3. Results

3.1 Construction and validation of the NPRGs prognostic signature in the TCGA cohort

Out of 67 NPRGs, Lasso regression analysis found six eligible candidate genes (Fig. 1A, B). The prognostic features were created using the expression level and risk coefficient of the six NPRGs as a guide: -0.50531*BRAF + 0.20844*PLK1 + 0.51169*TSC1 - 0.14410*AXL - 0.45049*ZBP1 + 0.28569*EGFR is the risk score. Risk scores were computed per the prognostic signature for each patient with melanoma. All patients in the TCGA cohort were split into high- or low-risk groups based on the risk score's median value. Patients in the low-risk category had a higher survival rate than those in the high-risk group, according to progression free survival (PFS) (Fig. 1C). Patients with the OS who fell into the low-risk category also had a higher survival rate than those who fell into the high-risk category (Fig. 1D). The diagnostic adequacy and sensitivity of the prognostic signature were also assessed using ROC curves, and ROC analysis revealed that the AUC at 1-, 3-, and 5-years survival were, respectively, 0.729, 0.671, and 0.711 (Fig. 1E). This proves that the prognostic signature we created has accurate OS prediction capacity. The expression levels of each NPRG in the high- and low-risk groups were displayed on the heat map. BRAF, AXL, and ZBP1 expression levels in the high-risk group were comparatively

ISSN 2618-1584 Vol. 7, Issue 5: 29-42, DOI: 10.25236/FMSR.2025.070505

low, but PLK1, TSC1, and EGFR expression levels were very high (Fig. 1F). The scatter dot plot of patients' risk scores in various categories showed that the high-risk area had a high number of fatalities (Fig. 1G, H).

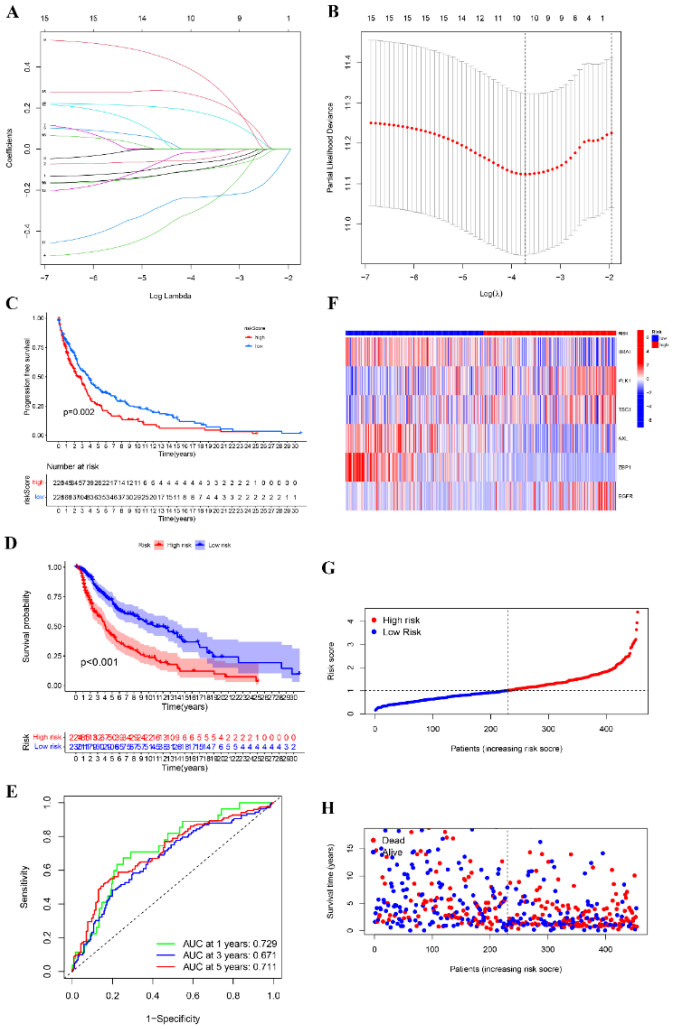

Fig.1 Construction and validation of the NPRGs prognostic signature in the TCGA cohort. (A) Diagram of the optimal number of genes in the LASSO regression model. The horizontal axis represented log (lambda), and the vertical axis represented the partial likelihood of deviance. The Lambda value corresponding to the minimum value was the best. (B) The coefficient spectrum of the LASSO Cox regression model. (C) K-M curves of progression-free survival (PFS). (D) K-M curves of overall survival (OS). (E) Receiver operating characteristic (ROC) curve for 1-, 3-, and 5-year overall survival. (F) Heat map for the expression levels of AXL, BRAF, EGFR, PLK1, TSC1, and ZBP1. (G) Risk score plot. (H) Survival status scatters the plot.

3.2 External validation of the prognostic signature

The independent validation cohort of the GEO database examined the prognostic signature for OS's ability to predict outcomes (GSE65904). The risk score's median value was used to categorize patients into low- and high-risk categories. The low-risk group had a higher rate of survival than those in the high-risk group, according to the KM survival curve (Fig. 2A). The diagnostic effectiveness of the prognostic signature was also assessed using ROC curves, and ROC analysis revealed that the AUC at 1-, 3-, and 5-years survival was, respectively, 0.676, 0.651, and 0.651. (Fig. 2B). Each gene's expression levels were similar to those of the TCGA cohort (Fig. 2E). The distribution of patients' risk assessments across several categories was ranked in Fig. 2C. The scatter dot plot also demonstrates that when a patient's score rises, the likelihood of death increases (Fig. 2D). Patients in the low-risk group saw fewer deaths than those in the high-risk group, according to the distribution of risk scores and the scatter dot plot.

ISSN 2618-1584 Vol. 7, Issue 5: 29-42, DOI: 10.25236/FMSR.2025.070505

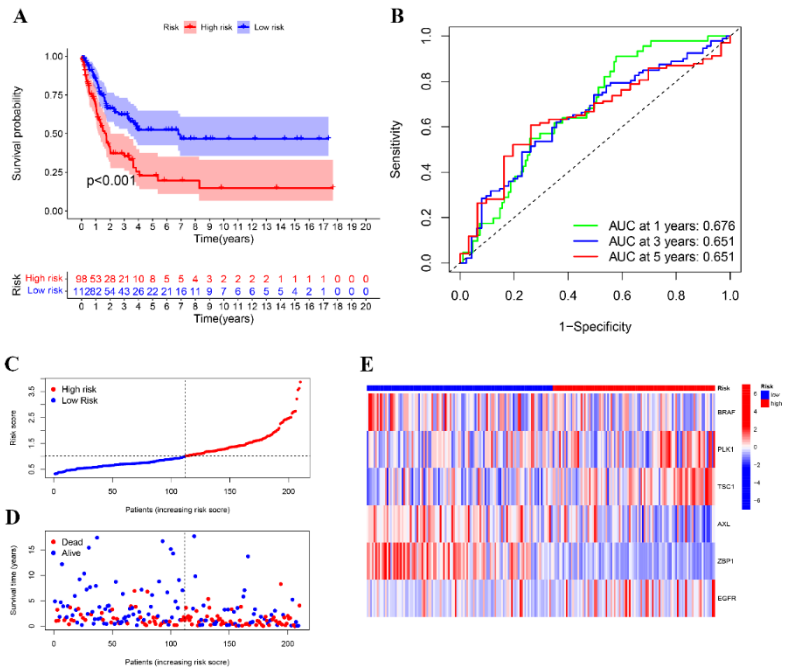

Fig.2 External validation of the NPRGs prognostic signature in the GEO cohort. (A) K-M curves of overall survival (OS). (B) Receiver operating characteristic (ROC) curve for 1-, 3-, and 5-year overall survival. (C) Risk score plot. (D) Survival status scatters the plot. (E) Heat map for the expression levels of AXL, BRAF, EGFR, PLK1, TSC1, and ZBP1.

3.3 Correlations between necroptosis scores and different clinical features

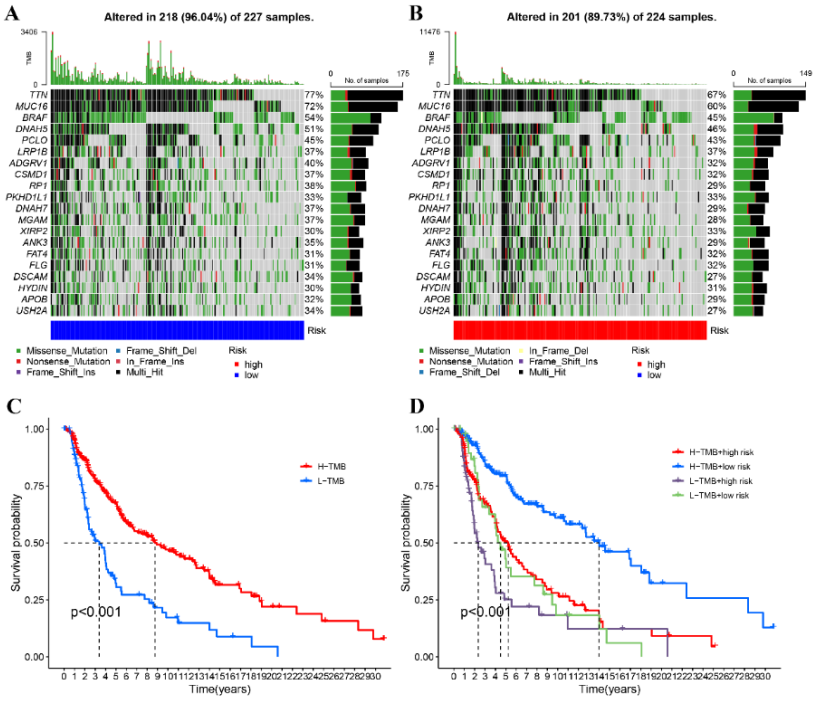

Fig.3 Correlation analysis between necroptosis scores and tumor mutation burden. (A) Waterfall plot of mutation profiles established in the low-risk groups. (B) Waterfall plot of mutation profiles established in the high-risk groups (C) Kaplan-Meier curves of the overall survival (OS) between high and low TMB groups. (D) Kaplan-Meier curves of the OS between high and low TMB groups stratified by necroptosis score.

ISSN 2618-1584 Vol. 7, Issue 5: 29-42, DOI: 10.25236/FMSR.2025.070505

We analyzed the distribution of the somatic mutations in the TCGA melanoma cohort between high and low necroptosis scores. The top 20 driver genes with the highest mutation frequencies and the associated mutation frequencies in the groups with high and low necroptosis scores (Fig. 3A, B). The TMB in the low necroptosis group was wider than in the group with high necroptosis scores. Patients were next split into two groups, one with high TMB and one with low TMB, based on the ideal cutoff. Patients in the high TMB cohort had a greater OS than those in the low, according to survival analysis (Fig. 3C). Next, we looked at how the synergistic TMB and necroptosis scores affected the prognosis of melanoma patients. TMB levels did not impact the independent predictive value of the necroptosis scores, according to a stratified survival study. There were significant variations between subclusters with high and low necroptosis scores for TMB. The OS was better in patients with high TMB compared to low TMB among those with high necroptosis scores. Likewise, in the group with low necroptosis scores, patients with high TMB had better OS than those with low TMB (Fig. 3D). These findings might offer new perspectives on immunotherapy in the context of necroptosis phenotypic regulation.

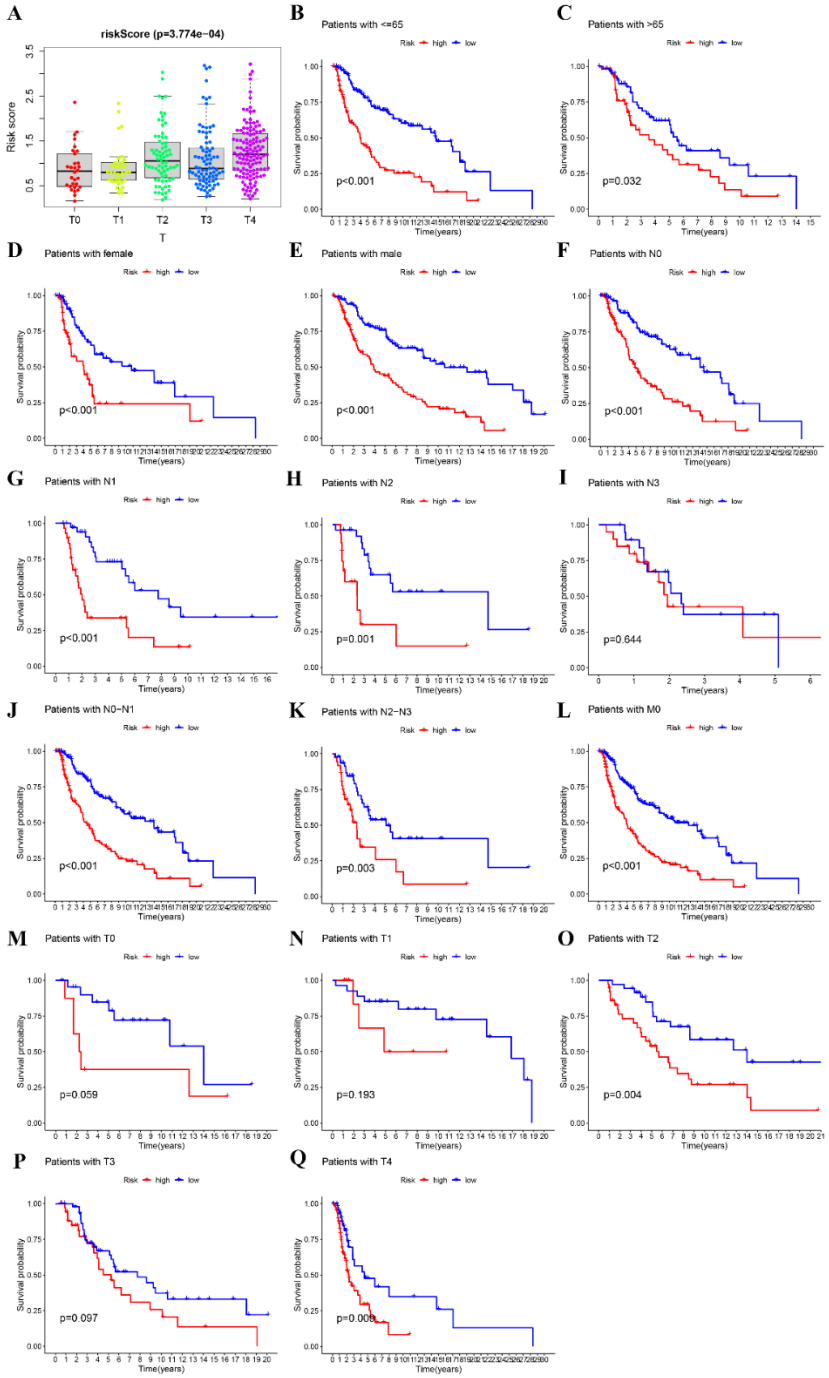

Fig.4 Correlations analysis between necroptosis scores and different clinical features.

ISSN 2618-1584 Vol. 7, Issue 5: 29-42, DOI: 10.25236/FMSR.2025.070505

In the TCGA cohort, the relationship between prognostic signature and clinicopathological characteristics was investigated. According to Fig. 4A, the risk score rises as the T phase progresses, indicating that the prognostic factors may be associated with tumor progression. Additionally, individuals with low scores had a significant survival benefit in the correlation study between necroptosis scores and other clinical parameters (age, sex, stage, and lymph node metastasis) (Fig. 4B-Q). Overall, the prognosis of long-term clinical patients can be predicted by the necroptosis scores.

3.4 The NPRGs prognostic signature independent of clinicopathological parameters in the TCGA cohort

In the TCGA cohort, we performed univariate and multivariate Cox regression analyses to see if the prognostic signature's predictive power depended on clinicopathological factors. The risk score was identified as a prognostic factor by univariate analysis [HR 1.513; % CI 1.297–1.766; (Fig. 5A)]. After adjusting for additional confounding variables, the multivariate analysis further showed that the risk score was an independent predictor for melanoma patients [HR 1.408; 95 % Ci 1.189–1.666; (Fig. 5B)].

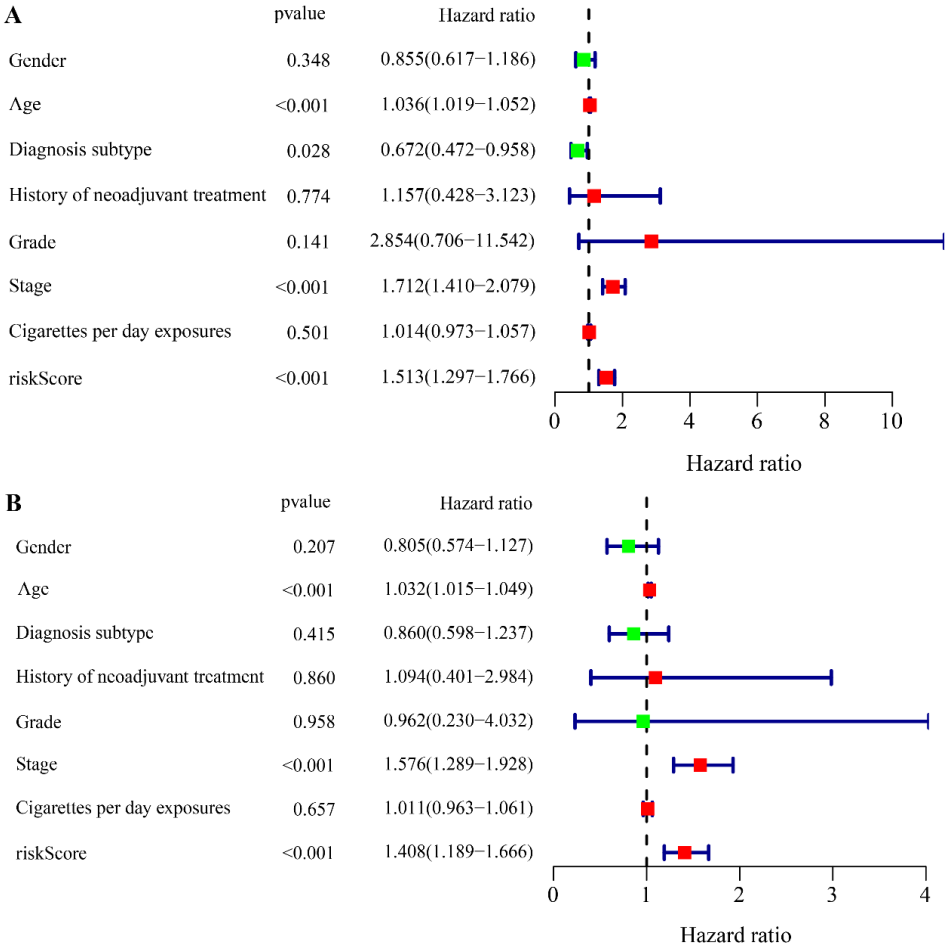

Fig.5 The NPRGs prognostic signature was an independent predictor for melanoma patients. (A) Forest plot of the univariate Cox regression analysis. (B) The forest plot of the multivariate Cox regression analysis.

3.5 Establishment of the nomogram

Based on the prognostic signature of the NPRG, we created a nomogram that might predict the survival of OS patients (Fig. 6A). To evaluate the nomogram's sensitivity and specificity, clinical ROC curves were employed. This nomogram's AUC was 0.742, indicating the nomogram may have clinical utility (Fig. 6B). Finally, by calibrating the curves, the prediction accuracy was evaluated (Fig. 6C). The aforementioned findings show that the nomogram has good accuracy for both internal and external validation datasets.

ISSN 2618-1584 Vol. 7, Issue 5: 29-42, DOI: 10.25236/FMSR.2025.070505

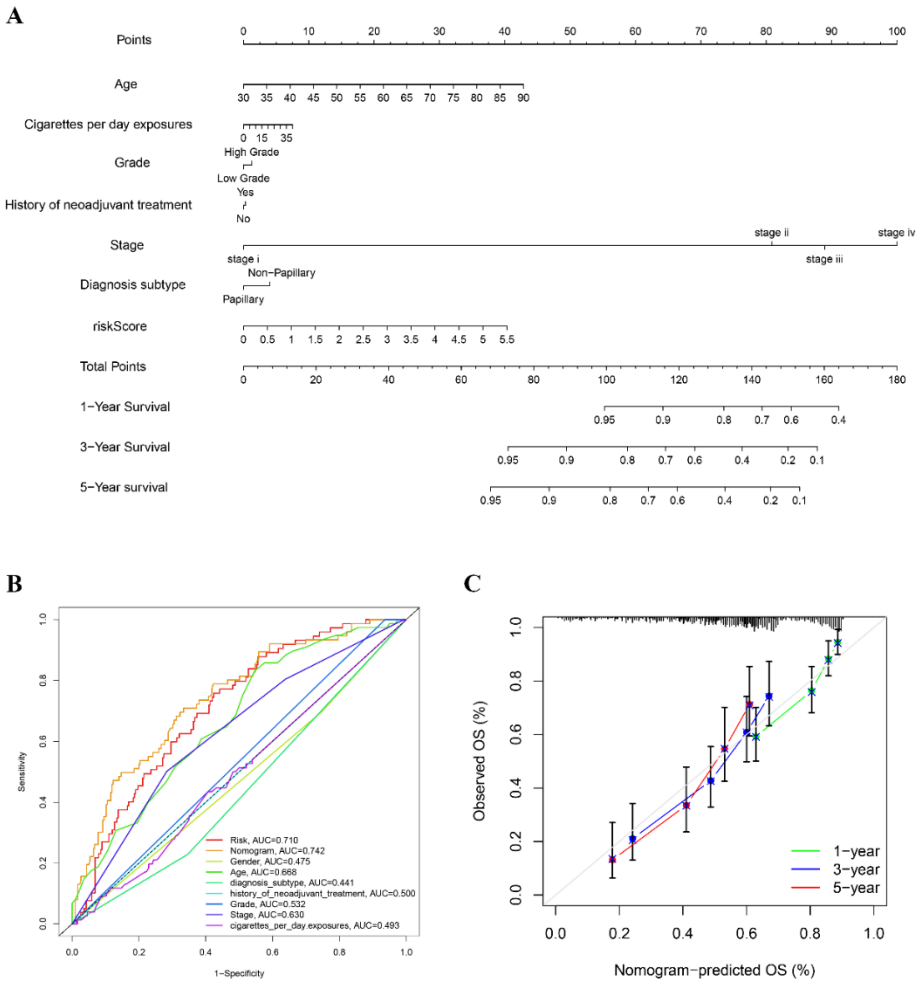

Fig.6 Establishment of the nomogram. (A) Nomogram for predicting 1-, 3-, and 5-year overall survival. (B) The clinical ROC curves of the nomogram. (C) The calibration curves for the validation of the nomogram.

3.6 Correlation of NPRGs prognostic signature with the proportion of TICs

22 different types of immune cell profiles were performed in melanoma patients to support further the relationship between the prognostic signature of the NPRG and the immunological microenvironment. The proportion of tumour-infiltrating immune subsets was also examined using the CIBERSORT algorithm (Fig. 7).

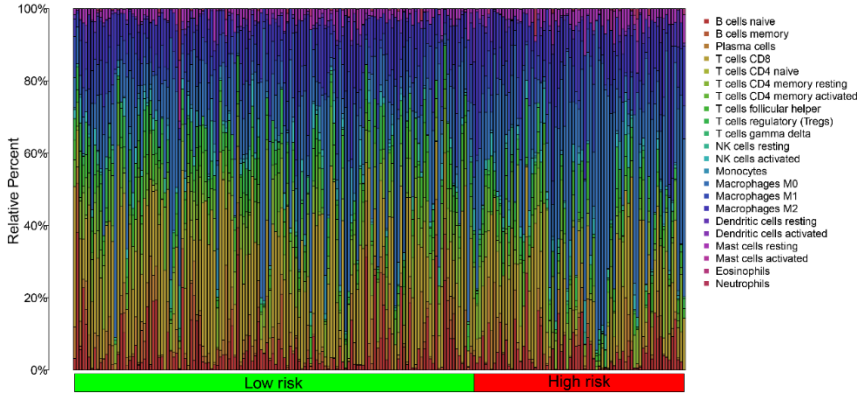

Fig.7 Barplot of the proportion of 22 kinds of tumor-infiltrating immune cells in melanoma samples.

ISSN 2618-1584 Vol. 7, Issue 5: 29-42, DOI: 10.25236/FMSR.2025.070505

Additionally, there is a strong correlation between the prognostic signature of the NPRG and the percentage of memory B cells (R=-0.25, P0.001), plasma cells (R=-0.21, P0.01), T cells CD8 (R=-0.3, P0.001), T cells CD4 memory activated (R=-0.23, P0.001), T cells follicular helper (R=-0.28, P0.001), natural killer (NK) cells resting (R=0.18, P<0.01) (Fig. 8A, B). These findings provide additional evidence for the influence of NPRG's prognostic signature on TME's immune activity.

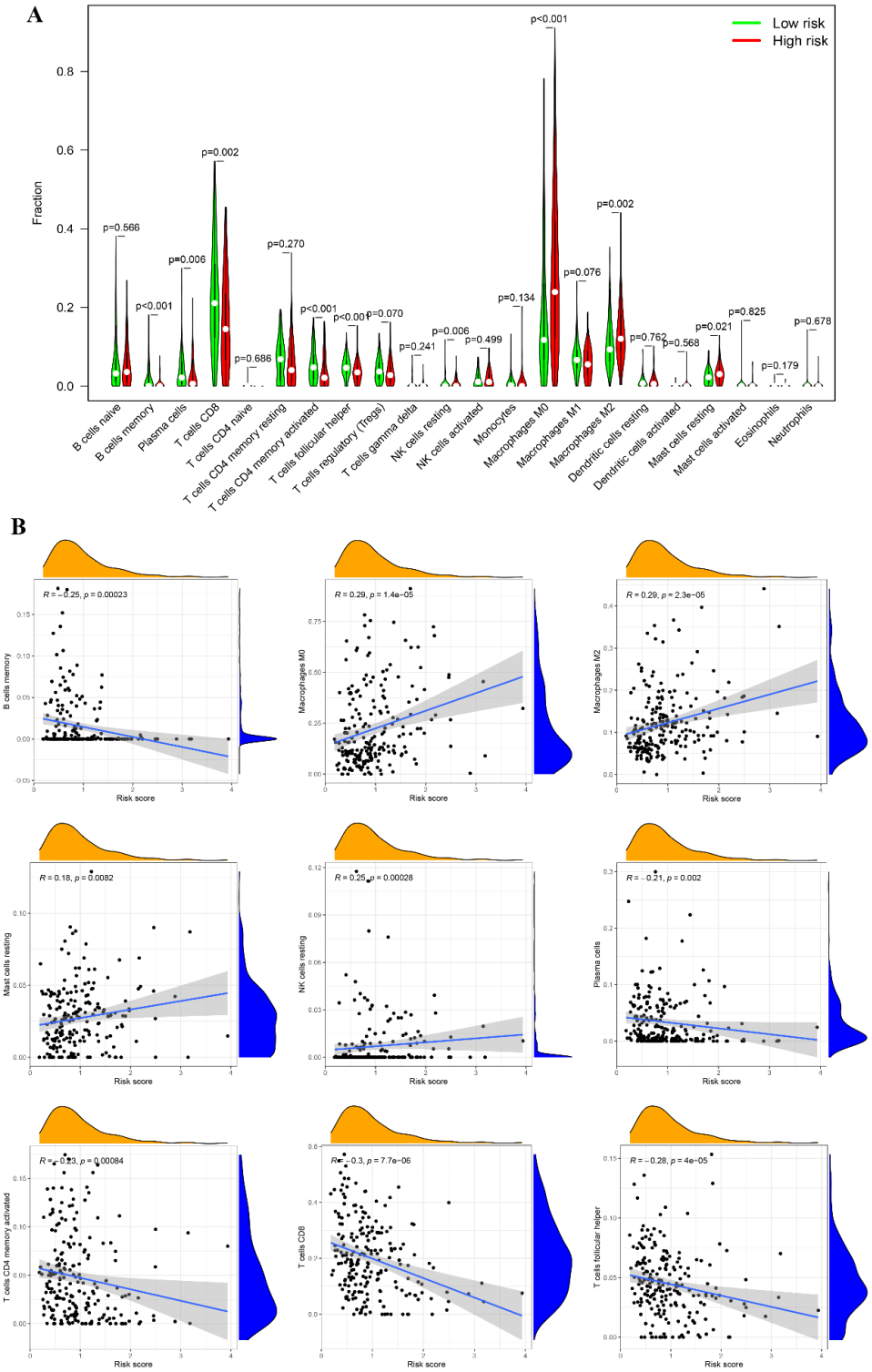

Fig.8 Tumor-infiltrating immune cells profile in melanoma samples and correlation analysis. (A) Violin plot showed the ratio differentiation of 22 kinds of immune cells with high and low risk. (B) Correlation analysis between necroptosis scores and immune cells.

ISSN 2618-1584 Vol. 7, Issue 5: 29-42, DOI: 10.25236/FMSR.2025.070505

3.7 Effectiveness prediction of immunotherapy and targeted therapy with the prognostic signature

The levels of mRNA expression for immunotherapy and targeted therapy in the high- and low-risk groups were compared (Fig. 9). The results showed that the low-risk group had significantly higher expression levels of CTLA4, CD40LG, CD40, CD274, etc. than the high-risk group did. Therefore, immunotherapy and targeted therapy may be less effective in melanoma patients with higher risk scores.

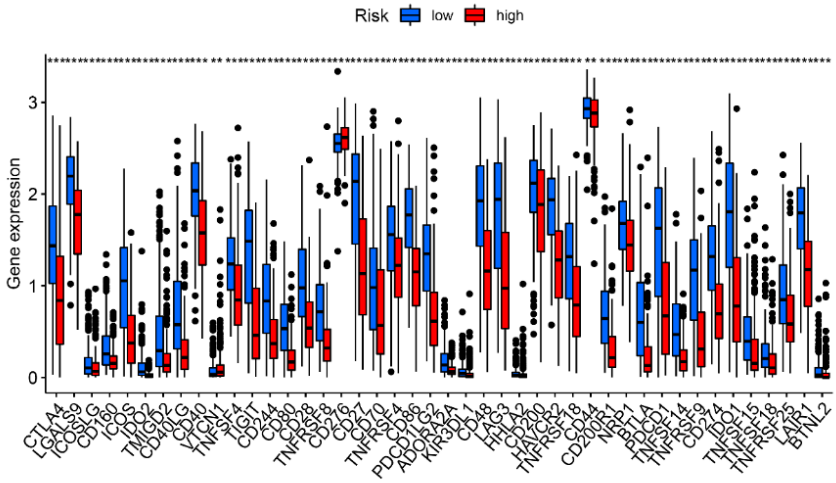

Fig.9 Expression of immune checkpoint-related genes in high-risk and low-risk groups.

3.8 Validation of the expression levels of six NPRGs

Based on the GEPIA2 database, we explored the mRNA expression levels of the six NPRGs on appeal, and the results showed that AXL, EGFR, and TSC1 were lowly expressed in melanoma patients' samples. At the same time, PLK1 was highly expressed (Fig. 10A). The immunohistochemistry results also validated the results (Fig. 10B).

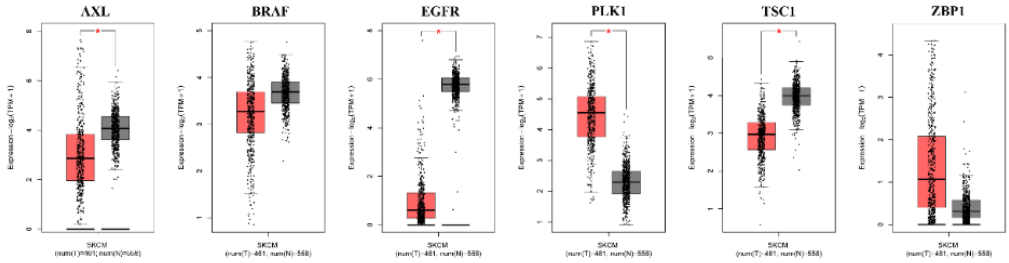

Fig.10 Validation of the expression levels of six NPRGs. (A) The mRNA expression levels of AXL, BRAF, EGFR, PLK1, TSC1, and ZBP1 are based on the GEPIA2 database. (B) Immunohistochemical staining in melanoma and paracancerous samples.

4. Discussion

We first analyzed the TCGA database's RNA transcriptome data in this study to obtain expression information for 67 NPRGs. Then, we built a predictive signature based on 6 NPRGs using LASSO regression in the TCGA cohort. The prognostic signature's superior predictive potential and accuracy were confirmed by internal validation based on the TCGA cohort. Additionally, the prognostic signature's predictive capability was examined in greater detail in a separate cohort of the GEO dataset, confirming its superior predictive ability for melanoma. We then discovered that necroptosis scores might be connected to tumour development. According to this interpretation, higher necroptosis scores are consistent with a worse tumour microenvironment, facilitating malignant cells' fast proliferation, invasion, and migration as tumours progress. The predictive signature was later demonstrated to represent prognostic factors independent of all clinicopathological characteristics in univariate and multivariate

ISSN 2618-1584 Vol. 7, Issue 5: 29-42, DOI: 10.25236/FMSR.2025.070505

Cox regression models. Last but not least, the relationship between the prognostic signature and the level of immune cell checkpoint expression partially explains how necroptosis influences the prognosis of melanoma patients. Further study on necroptosis in melanoma may be worthwhile.

Prognostic signature includes 6 NPRGs (AXL, BRAF, EGFR, PLK1, TSC1, ZBP1). These genes have been studied in detail in certain malignancies, including melanoma. AXL is a tyrosine kinase membrane receptor that signals through PI3K, MAPK, and PKC as well as other pathways. Studies have shown that AXL is frequently overexpressed and linked to metastasis and a poor prognosis in several human malignancies, including breast, lung, gastric, metastatic colon, and prostate tumours[10]. A substantial relationship between AXL expression and patient clinical outcomes was also found[11, 12]. As a result, abnormal AXL expression and activation are strongly linked to tumour development[13, 14]. It is well known that BRAF mutations in melanoma hinder the apoptotic process and tumour suppressor inactivation from promoting and maintaining carcinogenesis. About half of instances of melanoma have these mutations, particularly BRAF V600E, which accounts for 90% of all known BRAF mutations[15]. EGFR-related pathways often offer a potent signal for epithelial cell survival or proliferation[16]. However, when deregulated, the consequences of its overexpression are often detrimental. By triggering cellular responses that promote survival and anti-apoptosis, including enhanced proliferation, motility, angiogenesis, vascular mimicry, and invasiveness, EGFR can initiate tumorigenesis[17, 18]. PLK1 is essential for advancing the cell cycle, especially in mitosis, cytokinesis, and the G2-M checkpoint[19]. PLK1 is overexpressed in various cancer types, and studies have shown that its expression negatively correlates with overall disease-free survival[20]. PLK1 is considered a promising target for cancer therapy based on multiple studies[21]. A crucial part of the PI3K/AKT/mTOR signalling cascade in TSC1. Working with different regulatory molecules is essential for development, cell growth and proliferation, survival, autophagy, and cilia development. TSC1 has a tumour-suppressive role in several human malignancies, including liver, lung, bladder, breast, ovarian, and pancreatic cancers, according to recent studies[22]. In the innate immune response, ZBP1 encodes a Z-DNA binding protein that binds to exogenous DNA and triggers the production of type I interferon[23]. Increased ZBP1 expression has been seen in breast, ovarian, colon, and non-small cell lung cancers and is thought to be a distinctive marker for these cancers, according to studies[24-27]. To sum up, the six NPRGs that composed the prognostic signature strongly correlated with the growth of tumours. These NPRGs can accurately predict patient prognosis based on the generated NPRGs, and their prognostic signature may be linked to tumour growth. However, the precise functions of genes other than BRAF and molecular pathways in melanoma have only sometimes been investigated. Research on how NPRGs contribute to the development of cancer and tumours may be discussed in the following.

The prognostic profile of the NPRG, including T cells CD8, T cells CD4 memory activated, and T cells follicular helper, is strongly and adversely connected with the amount of T cell infiltration in TME, according to our results. Evidence for the crucial roles that effector T cells, memory T cells, and T cell differentiation play in tumour immune response is mounting[28]. Higher infiltrating T cell concentrations indicate a positive prognosis. Additionally, we saw a strong negative correlation between high necroptosis scores, the quantity of B-cell and plasma cells in the cell infiltration, and a positive correlation with M2 macrophages. B-cell enrichment was the best predictive indicator for patients' long-term survival[29]. According to a study, those with metastatic colorectal cancer with strong B-cell infiltration have longer OS and a significantly lower probability of the illness returning[30]. Additionally, better survival in metastatic melanoma was linked to the cohabitation of CD8 T cells and CD20 B cells[31]. M2 macrophages are immunosuppressive and contribute to stromal remodelling, thus favouring tumour growth[32, 33]. These findings support the notion that greater necroptosis scores currently indicate a poor prognosis for patients, partially explaining the relationship between the prognostic signature of the NPRG and prognosis. TME is intricate and interactive, though; variations in the level of immune cell infiltration at various stages of tumour growth may impact how quickly a tumour develops. Higher necroptosis scores were positively linked with NK cell infiltration in TME in the current investigation. Cytotoxic T cells are the primary immune cells capable of regulating tumour growth and mediating responses to cancer immunotherapy, even though many immune cells, including NK cells and macrophages, can demonstrate tumoricidal activity[34]. It is mainly due to their ability to recognize and kill malignant and infected cells [35]. Furthermore, it is impossible to overlook the dual function of B cells in tumour growth. As was already said, there is certain evidence that supports B cells' ability to prevent the spread of tumours, but overall, it is still unclear how B cells contribute to the immune response to tumours. B cells exhibit vital effector actions in addition to antibody production. According to experimental data, B cells inhibit and boost anti-cancer immune responses[36]. In conclusion, our findings suggest that necroptosis influences TME, but future research will need to clarify the precise mechanism.

Research on tumour immunology and molecular biology have been quite active, and immunotherapy

ISSN 2618-1584 Vol. 7, Issue 5: 29-42, DOI: 10.25236/FMSR.2025.070505

now offers new possibilities for treating tumours[37]. We further investigated the prognostic significance of NPRGs prognostic signature on the advantages of immunotherapy, given the vital importance of innovative immunotherapies in clinical treatment. We researched how high and low scores patients differed in their immune checkpoint-related gene expression. The findings revealed that the high necroptosis score group had reduced expression of various checkpoint genes, including CTLA4, PD-L1 (CD274), CD80, B7-H3 (CD276), CD40, and CD40L (CD40LG), among others. The type and degree of immune cell infiltration in TME are consistent. According to these findings, patients with high necroptosis scores may be resistant to tumour immunotherapy. Investigating how necroptosis affects melanoma may bring a new theoretical framework for subsequent treatment.

We give a preliminary analysis of the predictive power of NPRGs that might serve as the theoretical underpinning for further investigation. Our study does have several non-negligible limitations, though. First, our prognostic signature does not include other potential gene transcript expression profiles connected to OS in melanoma, which exclusively involves data analysis of NPRGs transcriptomics. Additionally, transcriptome analysis cannot pinpoint the precise molecular mechanism underlying necroptosis, necessitating additional proteomic or metabolomic research. Second, substantial prospective investigations must be conducted further to evaluate the prognostic signature's accuracy and stability. Finally, in vitro and in vivo tests are required to support our findings to fully comprehend the biological significance of this NPRG's prognostic signature in melanoma.

5. Conclusion

In conclusion, the NPRGs prognostic signature can be applied in clinical practice to evaluate the corresponding immune cell infiltration characteristics of NPRGs in each melanoma patient to identify candidates for immunotherapy and direct more efficient treatment approaches. In addition, it can also be used to assess the clinicopathological characteristics of melanoma patients, including age, gender, clinical stage, and tumour mutation burden. Similarly, the prognostic signature can be used as an independent biomarker to assess the prognosis of melanoma patients. In the future, our findings are expected to improve the response of melanoma patients to immunotherapy and provide precise strategies for immunotherapy candidates.

References

[1] Falcone I, Conciatori F, Bazzichetto C, Ferretti G, Cognetti F, Ciuffreda L, et al. Tumor Microenvironment: Implications in Melanoma Resistance to Targeted Therapy and Immunotherapy. Cancers. 12 (2020).

[2] Siegel R L, Miller K D, Fuchs H E, Jemal A. Cancer Statistics, 2021. CA: a Cancer Journal For Clinicians. 71 (2021).

[3] Yan J, Wan P, Choksi S, Liu Z-G. Necroptosis and tumor progression. Trends In Cancer. 8 (2022) 21-27.

[4] Hartman M L. Non-Apoptotic Cell Death Signaling Pathways in Melanoma. International Journal of Molecular Sciences. 21 (2020).

[5] Lawlor K E, Khan N, Mildenhall A, Gerlic M, Croker B A, D'Cruz A A, et al. RIPK3 promotes cell death and NLRP3 inflammasome activation in the absence of MLKL. Nature Communications. 6 (2015) 6282.

[6] Newton K. RIPK1 and RIPK3: critical regulators of inflammation and cell death. Trends In Cell Biology. 25 (2015) 347-353.

[7] Schumacher T N, Schreiber R D. Neoantigens in cancer immunotherapy. Science (New York, N.Y.). 348 (2015) 69-74.

[8] Wagner G P, Kin K, Lynch V J. Measurement of mRNA abundance using RNA-seq data: RPKM measure is inconsistent among samples. Theory In Biosciences = Theorie In Den Biowissenschaften. 131 (2012) 281-285.

[9] Mayakonda A, Lin D-C, Assenov Y, Plass C, Koeffler H P. Maftools: efficient and comprehensive analysis of somatic variants in cancer. Genome Research. 28 (2018) 1747-1756.

[10] Scaltriti M, Elkabets M, Baselga J. Molecular Pathways: AXL, a Membrane Receptor Mediator of Resistance to Therapy. Clinical Cancer Research : an Official Journal of the American Association For Cancer Research. 22 (2016) 1313-1317.

[11] Cardone C, Blauensteiner B, Moreno-Viedma V, Martini G, Simeon V, Vitiello P P, et al. AXL is a predictor of poor survival and of resistance to anti-EGFR therapy in RAS wild-type metastatic colorectal

ISSN 2618-1584 Vol. 7, Issue 5: 29-42, DOI: 10.25236/FMSR.2025.070505

cancer. European Journal of Cancer (Oxford, England : 1990). 138 (2020).
[12] Yu W, Ge X, Lai X, Lv J, Wang Y. The up-regulation of Axl is associated with a poor prognosis and promotes proliferation in pancreatic ductal adenocarcinoma. International Journal of Clinical and Experimental Pathology. 12 (2019) 1626-1633.
[13] Antony J, Huang R Y-J. AXL-Driven EMT State as a Targetable Conduit in Cancer. Cancer Research. 77 (2017) 3725-3732.
[14] Shen Y, Chen X, He J, Liao D, Zu X. Axl inhibitors as novel cancer therapeutic agents. Life Sciences. 198 (2018).
[15] Ascierto P A, Kirkwood J M, Grob J-J, Simeone E, Grimaldi A M, Maio M, et al. The role of BRAF V600 mutation in melanoma. Journal of Translational Medicine. 10 (2012) 85.
[16] Levantini E, Maroni G, Del Re M, Tenen D G. EGFR signaling pathway as therapeutic target in human cancers. Seminars In Cancer Biology. (2022).
[17] Minder P, Zajac E, Quigley J P, Deryugina E I. EGFR regulates the development and microarchitecture of intratumoral angiogenic vasculature capable of sustaining cancer cell intravasation. Neoplasia (New York, N.Y.). 17 (2015) 634-649.
[18] Prenzel N, Fischer O M, Streit S, Hart S, Ullrich A. The epidermal growth factor receptor family as a central element for cellular signal transduction and diversification. Endocrine-related Cancer. 8 (2001) 11-31.
[19] Zitouni S, Nabais C, Jana S C, Guerrero A, Bettencourt-Dias M. Polo-like kinases: structural variations lead to multiple functions. Nature Reviews. Molecular Cell Biology. 15 (2014) 433-452.
[20] Liu Z, Sun Q, Wang X. PLK1, A Potential Target for Cancer Therapy. Translational Oncology. 10 (2017) 22-32.
[21] Su S, Chhabra G, Singh C K, Ndiaye M A, Ahmad N. PLK1 inhibition-based combination therapies for cancer management. Translational Oncology. 16 (2022) 101332.
[22] Mallela K, Kumar A. Role of TSC1 in physiology and diseases. Molecular and Cellular Biochemistry. 476 (2021) 2269-2282.
[23] Huang Q F, Fang D L, Nong B B, Zeng J. Focal pyroptosis-related genes and are prognostic markers for triple-negative breast cancer with brain metastases. Translational Cancer Research. 10 (2021) 4845-4858.
[24] Gu L, Shigemasa K, Ohama K. Increased expression of IGF II mRNA-binding protein 1 mRNA is associated with an advanced clinical stage and poor prognosis in patients with ovarian cancer. International Journal of Oncology. 24 (2004) 671-678.
[25] Ioannidis P, Mahaira L, Papadopoulou A, Teixeira M R, Heim S, Andersen J A, et al. 8q24 Copy number gains and expression of the c-myc mRNA stabilizing protein CRD-BP in primary breast carcinomas. International Journal of Cancer. 104 (2003) 54-59.
[26] Ioannidis P, Trangas T, Dimitriadis E, Samiotaki M, Kyriazoglou I, Tsiapalis C M, et al. C-MYC and IGF-II mRNA-binding protein (CRD-BP/IMP-1) in benign and malignant mesenchymal tumors. International Journal of Cancer. 94 (2001) 480-484.
[27] Ross J, Lemm I, Berberet B. Overexpression of an mRNA-binding protein in human colorectal cancer. Oncogene. 20 (2001) 6544-6550.
[28] Zhang L, Yu X, Zheng L, Zhang Y, Li Y, Fang Q, et al. Lineage tracking reveals dynamic relationships of T cells in colorectal cancer. Nature. 564 (2018) 268-272.
[29] Petitprez F, de Reyniès A, Keung E Z, Chen T W-W, Sun C-M, Calderaro J, et al. B cells are associated with survival and immunotherapy response in sarcoma. Nature. 577 (2020) 556-560.
[30] Meshcheryakova A, Tamandl D, Bajna E, Stift J, Mittlboeck M, Svoboda M, et al. B cells and ectopic follicular structures: novel players in anti-tumor programming with prognostic power for patients with metastatic colorectal cancer. PloS One. 9 (2014) e99008.
[31] Cabrita R, Lauss M, Sanna A, Donia M, Skaarup Larsen M, Mitra S, et al. Tertiary lymphoid structures improve immunotherapy and survival in melanoma. Nature. 577 (2020) 561-565.
[32] Pan Y, Yu Y, Wang X, Zhang T. Tumor-Associated Macrophages in Tumor Immunity. Frontiers In Immunology. 11 (2020) 583084.
[33] Sousa S, Brion R, Lintunen M, Kronqvist P, Sandholm J, Mönkkönen J, et al. Human breast cancer cells educate macrophages toward the M2 activation status. Breast Cancer Research : BCR. 17 (2015) 101.
[34] Morvan M G, Lanier L L. NK cells and cancer: you can teach innate cells new tricks. Nature Reviews. Cancer. 16 (2016).
[35] Martínez-Lostao L, Anel A, Pardo J. How Do Cytotoxic Lymphocytes Kill Cancer Cells? Clinical Cancer Research : an Official Journal of the American Association For Cancer Research. 21 (2015) 5047-5056.
[36] Maibach F, Sadozai H, Seyed Jafari S M, Hunger R E, Schenk M. Tumor-Infiltrating Lymphocytes

ISSN 2618-1584 Vol. 7, Issue 5: 29-42, DOI: 10.25236/FMSR.2025.070505

and Their Prognostic Value in Cutaneous Melanoma. Frontiers In Immunology. 11 (2020) 2105.
[37] Wang S-D, Li H-Y, Li B-H, Xie T, Zhu T, Sun L-L, et al. The role of CTLA-4 and PD-1 in anti-tumor immune response and their potential efficacy against osteosarcoma. International Immunopharmacology. 38 (2016) 81-89.